Femtosecond laser writing of polarization devices for optical circuits in glass

Luís A. Fernandes[a,b], Jason R. Grenier[a], Peter R. Herman[a],
J. Stewart Aitchison[a] and Paulo V. S. Marques[b]

[a]Institute for Optical Sciences and the Department of Electrical and Computer Engineering
University of Toronto, 10 Kings College Road, Toronto, Ontario, M5S 3G4, Canada
[b]INESC-Porto, Departamento de Física e Astronomia da Universidade do Porto,
Rua do Campo Alegre 687, 4169-007 Porto, Portugal

ABSTRACT

In this paper we examine the birefringence of buried optical waveguides written with femtosecond lasers in bulk fused silica glass. We report two modes of low and high birefringence associated with strong form birefringence and the orientation of nanogratings that align perpendicular to the writing laser polarization. The birefringence and waveguide losses are characterized over various laser exposure conditions to facilitate the fabrication of low-loss and compact wave retarders and polarization beam splitters for integration into polarization controlled circuits. Zero-order quarter-wave and half-wave retarders together with polarization beam splitters are demonstrated, all operating at telecom wavelengths. Integration of such devices is targeted for application in photonic quantum circuits.

Keywords: Femtosecond laser, Laser direct writing, Integrated optics devices, Polarization-selective devices, Polarization beam splitters, Wave retarders.

1. INTRODUCTION

Waveguides fabricated in fused silica by femtosecond laser exposure have birefringence inherent to the anisotropy of the nonlinear absorption mechanisms in the non heat accumulation regime.[1–3] We can take advantage of this property for the fabrication of polarization dependent devices for a wide range of photonic applications.

In this paper we report two modes of low and high birefringence associated with strong form birefringence and the orientation of nanogratings[4,5] that align perpendicular to the writing laser polarization.[6] These nano structures have been exploited previously in the fabrication of diffraction gratings,[7] birefringent elements,[8] computer-generated holograms[9,10] and microfluidic devices.[11,12]

Laser exposure parameters were finely tuned to examine and optimize the birefringence of waveguides in order to control wave retardance and polarization dependent coupling with minimal optical losses in the 1250 nm to 1700 nm spectrum domain. These devices offer the possibility for three-dimensional integration[13] into quantum photonics systems.[14–16] We take advantage of the stability of the fused silica substrate and the scalability, versatility and compactness enabled by the femtosecond laser writing technique together with the new ability of inserting polarization devices to tailor the response of future optical circuits. Detailed analyses of the procedures and results are presented in this paper together with a review our most recent experimental findings.[17,18]

Further author information: (Send correspondence to Luís A. Fernandes)
Luís A. Fernandes: E-mail: lfernandes@fc.up.pt
Jason R. Grenier: E-mail: j.grenier@utoronto.ca
Peter R. Herman: E-mail: p.herman@utoronto.ca
J. Stewart Aitchison: E-mail: stewart.aitchison@utoronto.ca
Paulo V. S. Marques: E-mail: psmarque@fc.up.pt

Frontiers in Ultrafast Optics: Biomedical, Scientific, and Industrial Applications XII,
edited by Alexander Heisterkamp, Michel Meunier, Stefan Nolte, Proc. of SPIE Vol. 8247, 82470M

2. WAVEGUIDE FABRICATION

Waveguides were formed in fused silica glass by using a femtosecond laser writing technique. A Yb-doped fiber, chirped pulse amplified laser (IMRA America µJewel D-400-VR), generated 1044 nm center wavelength light with 300 fs pulse width and operated at 500 kHz repetition rate. The pulses were frequency doubled to 522 nm with a lithium triborate (LBO) crystal for second harmonic generation (SHG). Refractive index change was generated by focusing the femtosecond laser pulses with a 0.55 NA aspheric lens into a spot with a diameter of 1.6 µm ($1/e^2$ intensity), 75 µm below the surface of the fused silica substrate (Corning 7980, 50.8 mm × 25.4 mm × 1 mm with all faces optically polished). The high laser intensities reached in the focal volume drove nonlinear absorption in the glass and produced permanent refractive index changes in the material. To define the waveguides, the sample was scanned at a constant speed of 0.27 mm/s using an air-bearing motion stage (Aerotech ABL1000) with 2.5 nm of resolution. The waveguides were written with a length of 25.4 mm.

The polarization state of the writing laser with respect to the scanning direction was controlled with a half-wave plate to align either parallel (along the z-axis) or perpendicular (along the x-axis) as shown in Fig. 1. The laser polarization controls the orientation of laser generated nanogratings,[6] thus inducing a form birefringence that depends on the nanogratings orientation in respect to the waveguide direction.

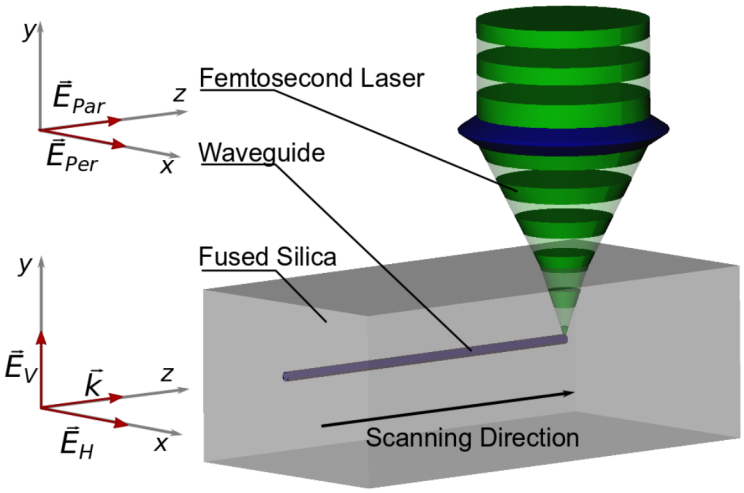

Figure 1. Fused silica substrate with focused femtosecond laser. The top axes represents the the polarizations of the writing laser (E_{Par} for parallel and E_{Per} for perpendicular in respect to the scanning direction). The bottom axes represents the proper polarization axes of the waveguides (V for vertical and H for horizontal).[18]

An acousto-optic modulator (AOM) in the laser path provided for modulation of the writing laser as previously described[19] and, therefore, formed segmented waveguides in a single step. By controlling the AOM frequency from 595 Hz to 470 Hz, Bragg grating waveguides (BGW) were formed that offered Bragg reflection peaks from 1300 nm to 1650 nm.

A range of exposure conditions, from 80 nJ to 200 nJ pulse energy and laser polarization parallel and perpendicular to the scanning direction, were studied. This processing window provided single mode waveguides with low loss in the telecom wavelength band from 1250 nm to 1700 nm.

Mode profiles were measured by coupling light from a tunable laser (Photonetics Tunics-BT) through a single mode fiber (SMF) into the waveguides and imaged onto a CCD camera (Spiricon SP-1550M) with a 60× magnification lens. This was done in order to assess the mode mismatch loss of the waveguides.

3. BIREFRINGENCE CHARACTERIZATION

The birefringence was characterized using free space coupling of light into the end facet of the waveguides using an aspheric objective lens (New Focus, 30×, 0.4 NA). The light exiting at the end of the waveguide was collected into either an optical spectrum analyzer (OSA) or a power meter. Polarization of the input and output light

was controlled by using two identical broadband polarizers (Thorlabs LPNIR). Two complementary methods were used to definitively determine the birefringence and its dependence on wavelength and exposure conditions. One method relied on measuring the spectral splitting of the Bragg wavelength peak (in a BGW) of the proper waveguiding modes and the other relied on using crossed polarizers with a uniform waveguide to determine the retardance created by the birefringence.

3.1 Bragg grating waveguide shift detection algorithm

The wavelength peak in the spectra produced by a BGW follows the Bragg relation $\lambda_B = 2n\Lambda$, where λ_B is the reflected Bragg wavelength, n is the effective index of the waveguiding mode and Λ is the periodicity of the grating structure. From the Bragg resonance peak it is possible to calculate the effective index of the mode. The birefringence is defined by the difference between the effective indexes of the proper modes (Vertical and Horizontal in this case) $\Delta n = n_V - n_H$. From the Bragg relation, the birefringence was determined using the difference between the Bragg wavelength peak in Equation 1.

$$\Delta n = \frac{\Delta\lambda_B}{2\Lambda} \tag{1}$$

For accurate determination of λ_B, the experimentally measured BGW transmission spectra for the two proper polarization modes were used. The two modes were prepared by adjusting the input polarizer and the transmission spectra was obtained by coupling the output light into the OSA. In Equation 2, $V(\lambda)$ and $H(\lambda)$ are the transmission spectra of a BGW for vertical and horizontal polarizations of the input light, $S(\Delta\lambda)$ is the square difference between the $H(\lambda)$ and $V(\lambda)$ transmission spectra as a function of a $\Delta\lambda$ shift of the H(Lambda) spectrum.

$$S(\Delta\lambda) = \sum_{\lambda=\lambda_{\min}}^{\lambda_{\max}} [V(\lambda) - H(\lambda + \Delta\lambda)]^2 \tag{2}$$

The wavelength difference between the $V(\lambda)$ and $H(\lambda)$ spectra, $\Delta\lambda_0$, was calculated with Equation 3 by determining the minimum of $S(\Delta\lambda)$. Fig. 2a shows the original spectra for $V(\lambda)$ and $H(\lambda)$ while Fig. 2b plots $S(\Delta\lambda)$ as a function of the wavelength shift applied to the $H(\lambda)$ spectrum.

$$\min[S(\Delta\lambda)] = S(\Delta\lambda_0) \tag{3}$$

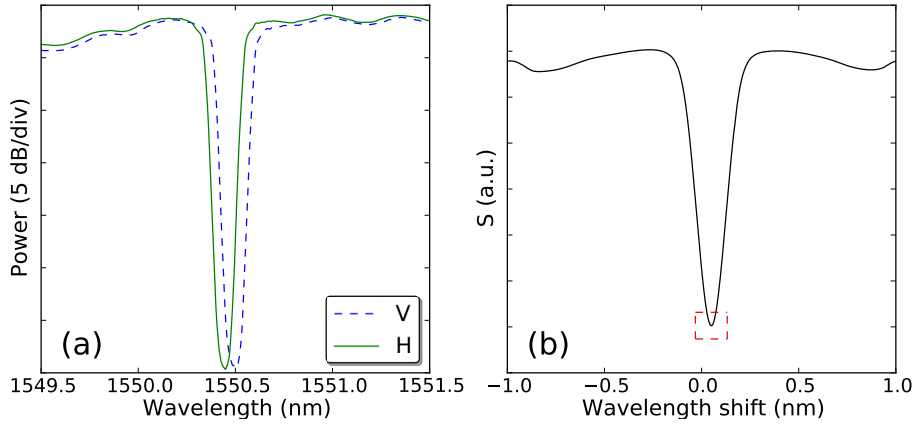

Figure 2. (a) Original BGWs transmission spectra for vertical and horizontal polarization probing. (b) Sum of the squared differences, $S(\Delta\lambda)$, from Equation 2.

For a more precise determination of $\Delta\lambda_0$, the three minimum points of $S(\Delta\lambda)$ (red box in Fig. 2b), were specified according to Equation 6 and plotted in Fig. 3a. The resolution of this measurement was further improved by calculating a correction factor, μ, defined in Equation 7, which interpolates between the discrete $S(\Delta\lambda)$ data provided by the OSA with the instrument limited step size being $\delta_\lambda = 0.002$.

$$S^- = S(\Delta\lambda_0 - \delta_\lambda) \tag{4}$$
$$S^+ = S(\Delta\lambda_0 + \delta_\lambda) \tag{5}$$
$$min(S) = S(\Delta\lambda_0) \tag{6}$$

$$\mu = \frac{S^- - S^+}{2[S^- + S^+ - 2S_{\min}]} \tag{7}$$

The best value for the wavelength shift, $\Delta\lambda_B$, was determined by Equation 8.

$$\Delta\lambda_B = \Delta\lambda_0 + \mu\delta_\lambda \tag{8}$$

This wavelength shift was added to the x-axis of the $H(\lambda)$ spectrum and plotted together with the unshifted $V(\lambda)$ spectrum in Fig. 3b to demonstrate the close overlapping of the the two spectra, confirming the accuracy of this method.

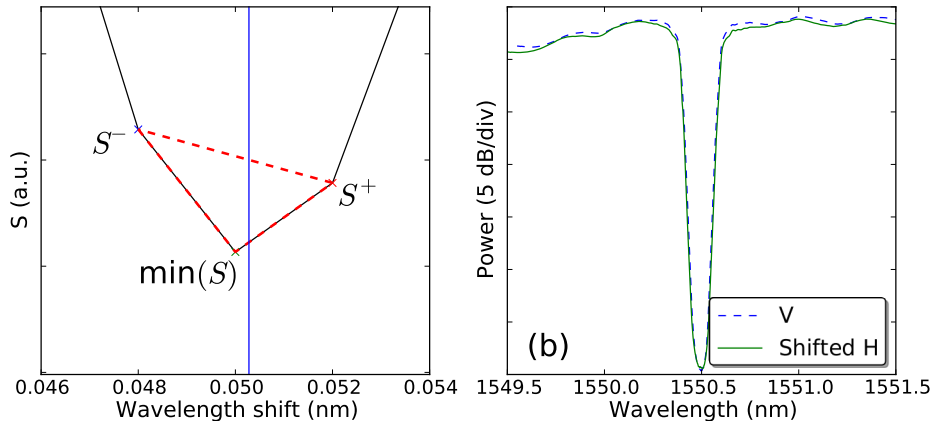

Figure 3. (a) Zoomed plot of the minimum of the sum of the squared differences showed in Fig. 2b. The vertical line represents the corrected minimum point of function $S(\Delta\lambda_0)$ used to determine $\Delta\lambda_B$. (b) BGWs transmission spectra for vertical and horizontal polarization with the horizontal polarization spectrum shifted by the best fitted value for birefringent wavelength shift, $\Delta\lambda_B$.

3.2 Cross polarizers technique

The Bragg grating waveguide shift method provides an absolute value of birefringence but only for a single wavelength. To explore the wavelength dependence of the birefringence, we found it favorable to use the cross polarizers technique. This method consists of recording the output power of a waveguide with an OSA for a broadband light source as an input and adjusting an input polarizer to be on a 45° angle with respect to the proper polarization axes. To measure the parallel power P_p and the crossed power P_c, an output polarizer was oriented to be 45° and -45°, respectively, with respect to the same axes as the input. The retardance δ was calculated with Equation 9. A more detailed explanation of this method can found in previous work.[18]

$$\delta = \pm \arccos(P_p - P_c) + m2\pi \tag{9}$$

The birefringence, Δn, is related to the retardance by Equation 10, where L is the length of the waveguide and m is an integer that represents the retardance order.

$$\Delta n = \frac{\delta\lambda}{2\pi L} \tag{10}$$

The birefringence results obtained from these measurements were indeterminate because of the $\pm$ sign in the arccosine function and the ambiguity in the $m2\pi$ term. These ambiguities could be resolved by consolidating the results with the absolute values of birefringence obtained by the Bragg grating waveguide shift method. Fig. 4 shows, as an example, the solutions of Equation 10 for the case of perpendicular polarization of the writing laser with 160 nJ of pulse energy and for m between 2 and 5. The red circles (●) represent the results obtained using four BGW with different periodicity and indicate the correct choice for the birefringence from the cross polarizers method as highlighted by the broadened yellow line.

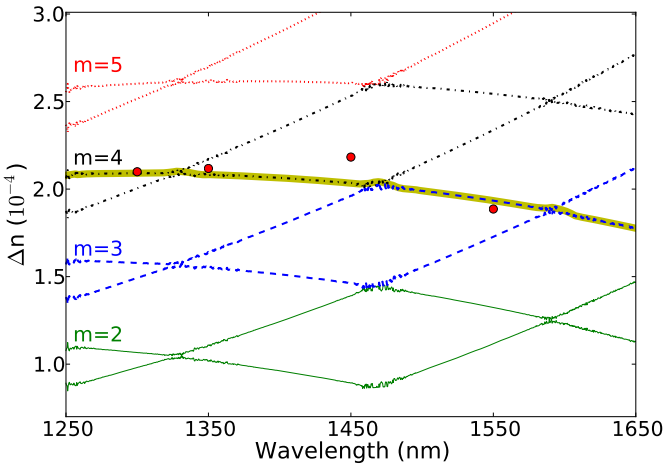

Figure 4. Results from the cross polarizers method and for the Bragg grating waveguide shift method for a 25.4 mm waveguide. The various lines represent the ambiguous birefringence values obtained from the cross polarizers method, with values of m equal to 2, 3, 4, and 5. Each of these is split into two lines due to the $\pm$ sign ambiguity of the arccosine function. The red circles (●) represent the results obtained using four BGWs. The highlighted line is the correct birefringence result.

4. RESULTS

The characterization methods presented in Section 3 provided the tools required to unambiguously analyze the birefringence dependence as a function of wavelength and laser writing condition which is summarized in the graph in Fig. 5. These results clearly demonstrate that the perpendicular polarization of the writing laser, which produces a parallel orientation of the nanogratings structures with respect to the waveguide, offers an order of magnitude higher birefringence than the parallel laser polarization condition. However, this writing orientation also produces higher modal mismatch and propagation losses in the waveguides as outlined in Table 1.

Table 1. Waveguide properties for 160 nJ pulse energy.

Writing laser polarization	Birefringence	Mismatch loss	Prop. loss, α
Parallel	$\approx 10^{-5}$	0.09 dB	0.6 dB/cm
Perpendicular	$\approx 10^{-4}$	0.14 dB	1.9 dB/cm

Using the results in Table 1, we were able to calculate the length required for a zero-order half-wave plate and the losses of such a waveguide. As shown in Table 2, the losses versus birefringence trade-of is favorable for

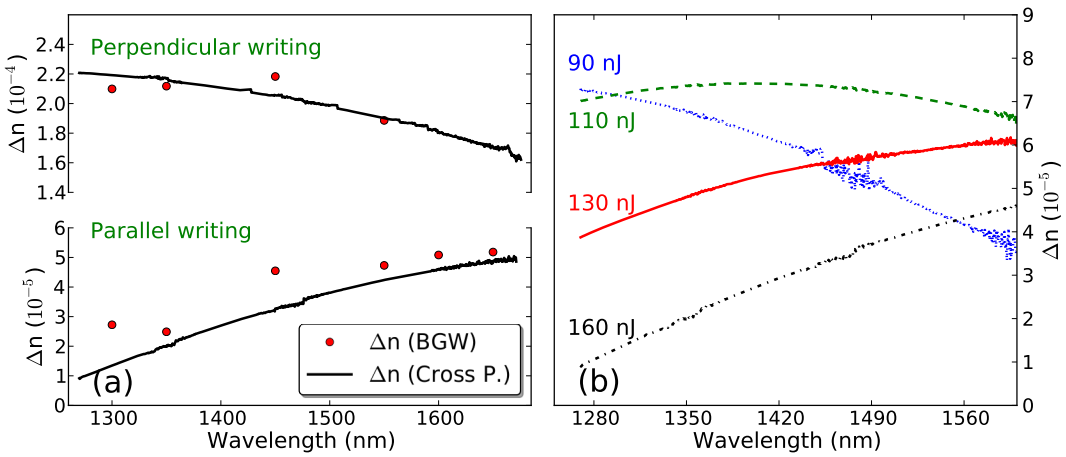

Figure 5. Birefringence as a function of the wavelength for (a) perpendicular and parallel polarizations of the writing laser with 160 nJ pulse energy and (b) different laser pulse energies for parallel polarized writing laser.[18]

the case of perpendicular polarization of the writing laser, allowing the fabrication of shorter (4 mm) wave plates with 0.7 dB lower losses than the longer (25.4 mm) wave plates required with in the parallel polarization case.

Table 2. Zero order ($m = 0$) half-wave plates @ 1550 nm.

Writing laser polarization	Waveguide length	Total insertion loss
Parallel	25.4 mm	1.5 dB
Perpendicular	4 mm	0.8 dB

4.1 Integrated wave plates

Based on the birefringence results shown in Fig. 5b it was possible to design waveguides to operate as quarter-wave or half-wave plates for a given wavelength. Fig. 6 shows the transmitted waveguide power as a function of the analyzer angle for a 25.4 mm length waveguide, probed with 45° linear polarized light and measured at two different wavelengths. At 1513 nm the waveguide operates as a half-wave plate, producing linear polarized light oriented at -45° and with 35 dB of polarization contrast. At 1365 nm the waveguide operates as a quarter-wave plate, producing elliptically polarized light with 5% variation from the ideal circular polarized output.

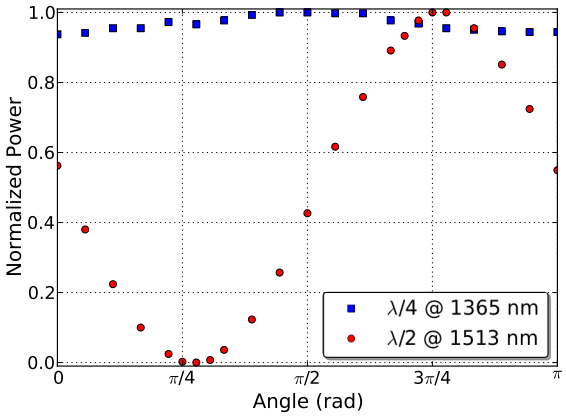

Figure 6. Quarter (■ blue square) and half (● red circle) wave plate operation as a function of the analyzer angle for a 25.4 cm long waveguide retarder, fabricated with 160 nJ of pulse energy and the writing laser polarized parallel with respect to the scanning direction.[18]

4.2 Polarization beam splitter

The birefringence present in these waveguides produces a polarization dependent coupling coefficient when a directional coupler is designed as shown in Fig. 7. This will in turn produce a polarization dependent coupling ratio which can be used to fabricate an integrated polarization beam splitter. The detailed fabrication and device characterization as been previously presented.[17]

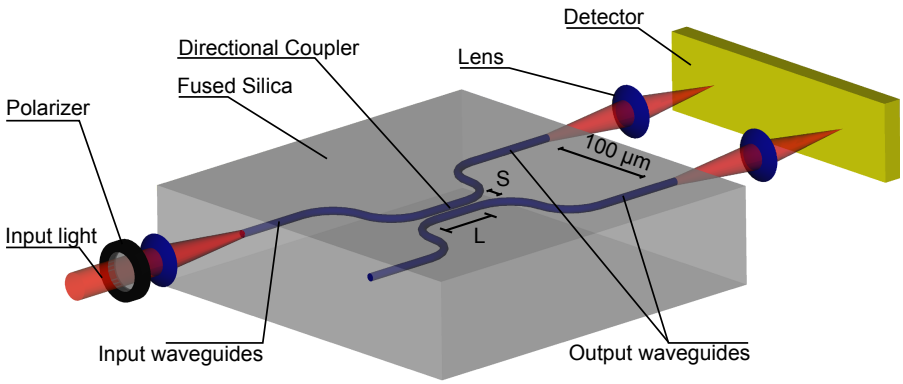

Figure 7. Polarization beam splitters schematics, identifying the coupling length, L, and the waveguide separation, S.[20]

Polarization beam splitter operation was demonstrated (Fig. 8) at 1484 nm for a directional coupler with a coupling length L of 19.2 mm and waveguide separation S of 8 µm. The ratio of power in respect to the input power measured in the detector in the same coupler arm as the input is P_1 and the power ratio measured in the opposite arm is P_2. This design demonstrated a 19 dB polarization extinction ratio for H polarized light when probed with V and -24 dB extinction ratio for the opposite case.

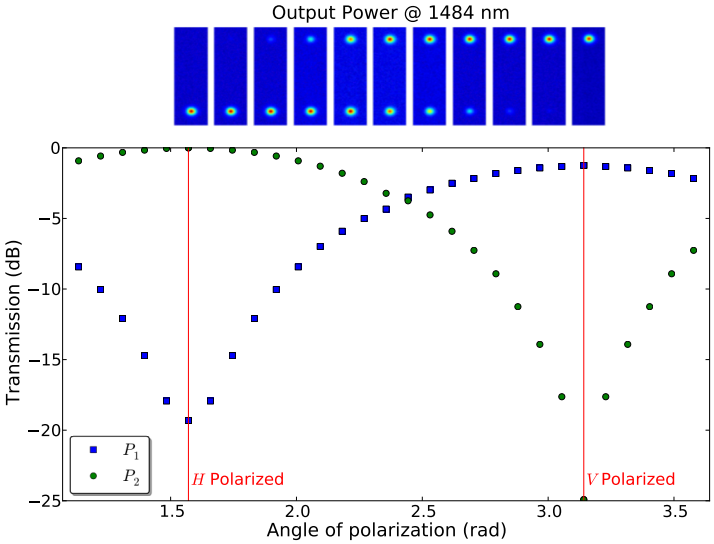

Figure 8. Directional coupler operating as a polarization beam splitter. Measured output power and mode profile as a function of the angle of polarization 1484 nm probing wavelength, (P_1, ● green circle) for the same arm as the input and (P_2, ■ blue square) for the opposite arm as the input.[17]

5. CONCLUSIONS

The waveguide birefringence produced by the femtosecond laser writing process was accurately measured by noting the polarization splitting of stopbands between proper polarization modes in Bragg grating waveguides, together with the cross polarization transmission study of uniform waveguides. Birefringence values ranged from 10^{-5}, for parallel, to 10^{-4} for perpendicular polarization of the writing laser. The trade-off between losses and birefringence was explored in order to find optimized fabrication parameters for these devices. Zero-order retarders were demonstrated with 5% variation from ideal circular polarized light for a quarter-wave retarder and 35 dB linear polarization contrast ratio for a half-wave retarder. A polarization beam splitter was demonstrated with polarization splitting contrast ratios of -19 dB and -24 dB.

ACKNOWLEDGMENTS

The authors would like to acknowledge the Natural Sciences and Engineering Research Council of Canada and Canadian Institute for Photonic Innovations for the financial support of this project. Luís Fernandes would also like to acknowledge the Portuguese Fundação para a Ciência e Tecnologia for his Ph.D Fellowship.

REFERENCES

[1] Bellouard, Y., Colomb, T., Depeursinge, C., Dugan, M., Said, A., and Bado, P., "Nanoindentation and birefringence measurements on fused silica specimen exposed to low-energy femtosecond pulses," *Optics Express* **14**(18), 8360–8366 (2006).

[2] Bhardwaj, V., Corkum, P., Rayner, D., Hnatovsky, C., Simova, E., and Taylor, R., "Stress in femtosecond-laser-written waveguides in fused silica," *Optics Letters* **29**(12), 1312–1314 (2004).

[3] Yang, P., Burns, G., Guo, J., Luk, T., and Vawter, G., "Femtosecond laser-pulse-induced birefringence in optically isotropic glass," *Journal of Applied Physics* **95**, 5280 (2004).

[4] Bricchi, E., Klappauf, B., and Kazansky, P., "Form birefringence and negative index change created by femtosecond direct writing in transparent materials," *Optics Letters* **29**(1), 119–121 (2004).

[5] Richter, S., Heinrich, M., Döring, S., Tünnermann, A., and Nolte, S., "Formation of femtosecond laser-induced nanogratings at high repetition rates," *Applied Physics A: Materials Science & Processing* **104**(2), 503–507 (2011).

[6] Taylor, R., Hnatovsky, C., Simova, E., Rajeev, P., Rayner, D., and Corkum, P., "Femtosecond laser erasing and rewriting of self-organized planar nanocracks in fused silica glass," *Optics Letters* **32**(19), 2888–2890 (2007).

[7] Beresna, M. and Kazansky, P. G., "Polarization diffraction grating produced by femtosecond laser nanostructuring in glass," *Optics Letters* **35**, 1662–1664 (May 2010).

[8] Ramirez, L., Heinrich, M., Richter, S., Dreisow, F., Keil, R., Korovin, A., Peschel, U., Nolte, S., and Tünnermann, A., "Tuning the structural properties of femtosecond-laser-induced nanogratings," *Applied Physics A* **100**(1), 1–6 (2010).

[9] Cai, W., Libertun, A., and Piestun, R., "Polarization selective computer-generated holograms realized in glass by femtosecond laser induced nanogratings," *Optics Express* **14**(9), 3785–3791 (2006).

[10] Papazoglou, D. and Loulakis, M., "Embedded birefringent computer-generated holograms fabricated by femtosecond laser pulses," *Optics Letters* **31**(10), 1441–1443 (2006).

[11] Hnatovsky, C., Taylor, R., Simova, E., Bhardwaj, V., Rayner, D., and Corkum, P., "Polarization-selective etching in femtosecond laser-assisted microfluidic channel fabrication in fused silica," *Optics letters* **30**(14), 1867–1869 (2005).

[12] Bellouard, Y., Said, A., Dugan, M., and Bado, P., "Fabrication of high-aspect ratio, micro-fluidic channels and tunnels using femtosecond laser pulses and chemical etching," *Optics express* **12**(10), 2120–2129 (2004).

[13] Nolte, S., Will, M., Burghoff, J., and Tuennermann, A., "Femtosecond waveguide writing: a new avenue to three-dimensional integrated optics," *Applied Physics A* **77**(1), 109–111 (2003).

[14] Marshall, G., Politi, A., Matthews, J., Dekker, P., Ams, M., Withford, M., and O'Brien, J., "Laser written waveguide photonic quantum circuits," *Optics Express* **17**(15), 12546–12554 (2009).

[15] Sansoni, L., Sciarrino, F., Vallone, G., Mataloni, P., Crespi, A., Ramponi, R., and Osellame, R., "Polarization entangled state measurement on a chip," *Physical review letters* **105**(20), 200503 (2010).
[16] Sansoni, L., Sciarrino, F., Vallone, G., Mataloni, P., Crespi, A., Ramponi, R., and Osellame, R., "Two-particle bosonic-fermionic quantum walk via integrated photonics," *Physical review letters* **108**(1), 010502 (2012).
[17] Fernandes, L. A., Grenier, J. R., Herman, P. R., Aitchison, J. S., and Marques, P. V. S., "Femtosecond laser fabrication of birefringent directional couplers as polarization beam splitters in fused silica," *Optics Express* **19**(13), 11992–11999 (2011).
[18] Fernandes, L., Grenier, J., Herman, P., Aitchison, J., and Marques, P., "Femtosecond laser writing of waveguide retarders in fused silica for polarization control in optical circuits," *Optics Express* **19**(19), 18294–18301 (2011).
[19] Zhang, H., Eaton, S., and Herman, P., "Single-step writing of bragg grating waveguides in fused silica with an externally modulated femtosecond fiber laser," *Optics Letters* **32**(17), 2559–2561 (2007).
[20] Fernandes, L., Grenier, J., Herman, P., Aitchison, J., and Marques, P., "Escrita de dispositivos ópticos integrados com laser de femtosegundos," *Gazeta de Física* **34**(1), 17–21 (2011).